International Journal of
Automotive Manufacturing and Materials (IJAMM)

Scilight

Article

Wall-Impingement Characteristics and Near-Wall Flow Dynamics of Diesel/Methanol Dual-Fuel Sprays under High Pressure

Haiming Sun [1], Zunhua Zhang [2,3], Chujun Luo [1], Mingfei Lu [2,*], Yangwanqing Yu [1], Dongsheng Dong [2,3], Xiangjie Zhang [2], and Yuming Zhang [2]

[1] China Gezhouba Group Co., Ltd., Wuhan 430033, China
[2] School of Naval Architecture, Ocean and Energy Power Engineering, Wuhan University of Technology, Wuhan 430063, China
[3] Hubei Engineering Research Center for Water Application of New Energy & Green Technology, Wuhan 430063, China
* Correspondence: Lu_MF1997@whut.edu.cn
Received: 28 November 2025; Revised: 23 March 2026; Accepted: 24 March 2026; Published: 2 April 2026

Abstract: The adoption of diesel/methanol dual direct injection has emerged as an effective strategy for reducing greenhouse gas and pollutant emissions in marine engines. However, dual-fuel sprays in the cylinder exhibit complex interaction, mixing, and wall-impingement behaviors. The high in-cylinder ambient pressure further intensifies liquid-wall and inter-spray dynamics. To clarify these effects, this study examines the wall-impingement characteristics of diesel/methanol dual-fuel sprays in a high-pressure constant-volume chamber. Shadowgraph imaging and quantitative analysis were used to resolve the evolution of spreading radius and uplift height under varying impingement distances and angles. Larger impingement distances enhance pre-impingement vapor formation and post-impact atomization, while reducing early-stage spreading and uplift. Increasing the impingement angle enhances the wall-guided deflection of the spray and shifts the gas-phase region from the methanol side toward the frontal vortex. Variations in impingement distance modify the balance between spray-wall and inter-spray interaction. In contrast, the impingement angle exerts a notably stronger influence on dual-fuel spray dynamics than methanol alone.

Keywords: diesel/methanol dual fuel; dual direct injection; spray characteristics; spray-wall impingement

1. Introduction

The global shipping industry is under increasing pressure to reduce emissions, and greenhouse gas and air pollutant emissions from ships have become central issues for the sector [1–3]. As a result, clean combustion technologies and low-carbon fuels are attracting growing attention. Among the available alternative fuels, methanol is considered a promising low-carbon option for internal combustion engines. It can be produced from different feedstocks, is stored and transported easily as a liquid at ambient conditions, and leads to relatively low carbon emissions [4–6]. However, the low heating value and poor auto-ignition characteristics of methanol limit its direct use in compression-ignition engines [7,8]. A highly reactive fuel such as diesel is usually required to ensure stable ignition, making diesel/methanol dual direct injection a practical approach that combines technical feasibility with cleaner emission performance [9,10].

To support the development of such combustion strategies, many studies have examined the spray characteristics of methanol under different injection and ambient conditions [11]. Overall, compared with diesel, methanol generally exhibits shorter penetration, a larger cone angle, and more irregular macroscopic boundaries under similar conditions, which has been consistently observed across constant-volume and high-pressure direct-injection studies [12–14].

On this basis, recent studies have begun to focus on diesel/methanol dual-fuel sprays to clarify how the interaction between the two fuels affects spray development and mixture formation. Compared with single-fuel methanol injection, where only fuel-air interaction occurs, diesel/methanol dual-fuel sprays involve plume-plume collision and mutual entrainment, making the injection process more complex. Using a shadowgraph method, Wang et al. [15] showed that very short injection intervals lead to obvious collision between diesel and methanol

plumes, whereas longer intervals allow the diesel spray to evaporate before methanol injection and thus eliminate direct interaction. Chen et al. [14] further reported that higher injection pressure and appropriate injection intervals markedly promote evaporation and atomization of diesel/methanol combined sprays and enlarge the overall spray area. Similar sensitivities of spray development to injection strategy and operating conditions have also been observed in optical studies of diesel-ignited methanol direct injection and methanol/diesel dual-fuel operation in optical engines [16,17]. Collectively, these studies highlight the mutual interaction between diesel and methanol sprays and provide a basis for further analysis of mixture formation and wall-impingement behavior.

Modern diesel engines commonly employ high fuel injection pressures [18–20]. However, higher injection pressure also increases spray penetration, so that in the later stage of injection the jet can impinge on the piston crown and cylinder liner, forming locally over-rich mixtures near the wall and thus increasing unburned hydrocarbon and soot emissions [21–23]. The near-wall fuel distribution, therefore, has a strong impact on the subsequent combustion process, making a clear understanding of spray-wall interaction essential for controlling in-cylinder mixture formation.

Extensive optical investigations of spray-wall interaction have primarily focused on diesel and diesel-like fuels. Li et al. [24] analyzed diesel spray-wall interaction and post-impingement mixture formation, and proposed a three-region structure consisting of the impingement zone, wall-jet spreading zone, and leading-vortex region. Allocca et al. [25] used schlieren imaging to study a GDI spray impacting a heated wall and showed that wall temperature has little influence on the liquid-phase width and thickness after impingement. Yu et al. [26] employed high-speed imaging to examine n-butanol/diesel blended sprays and found, based on a contribution index, that impingement distance and ambient pressure have the strongest effect on spread radius, while their influence on uplift height is weaker. Du et al. [27] further reported that higher injection pressure and larger nozzle orifice diameter enhance the radial spreading of gas- and liquid-phase diesel sprays after wall impingement, whereas the post-injection growth of spread radius is almost unaffected by these parameters.

More recently, Wang et al. [28] showed for n-dodecane that variations in wall temperature do not cause significant changes in macroscopic gas-phase spray parameters after impingement, while Liu et al. [29] visualized wall-impinging sprays under marine diesel engine conditions and demonstrated that higher ambient pressure enhances entrainment and droplet evaporation, leading to a larger uplift height along the wall. Compared with diesel, research on methanol spray-wall interaction is still limited. Zhang et al. [30] investigated low-pressure methanol sprays and found that increasing impingement distance changes the pre-impact spray shape from conical to cylindrical and reduces both spread radius and uplift height.

Overall, existing studies show that spray-wall interaction is highly sensitive to operating and geometric conditions, and that most work to date has focused on single-fuel diesel or surrogate sprays; in contrast, diesel/methanol dual-fuel wall-impinging sprays have rarely been addressed, even though the interaction between the two plumes is expected to make the impingement process more complex. Motivated by this gap, this study investigates wall-impinging sprays in a diesel/methanol dual-injection configuration in a constant-volume chamber under engine-relevant high-pressure conditions. The analysis focuses on the effects of wall-impingement distance and impingement angle on the evolution of spreading radius and uplift height, as well as on the inter-spray interaction. These findings clarify near-wall dispersion and inter-spray interaction of diesel/methanol sprays under high-pressure conditions. They provide a basis for future studies on mixture formation and combustion control in methanol/diesel dual direct-injection engines.

2. Experimental Method

2.1. Constant-Volume Chamber and Optical System

A high-pressure constant-volume chamber was used to visualize the development and wall-impingement behavior of diesel/methanol dual-fuel sprays under controlled conditions, as illustrated in Figure 1. The chamber is a cubic vessel made of 304 stainless steel, and its structural layout is presented in Figure 2. Each of the six faces is machined with a stepped opening (120 mm inner diameter, 160 mm outer diameter) for mounting fuel injectors, gas connections, or optical windows, which are sealed and fastened using bolt-clamped flanges. The top face accommodates a metal plug carrying the diesel and methanol injectors, as well as ports for pressure and temperature sensors. Two side faces are equipped with quartz optical windows to provide optical access for the imaging light path. The remaining faces are closed with metal plugs that incorporate intake and exhaust connections. Twelve brass heating blocks distributed along the chamber edges enable temperature control. Additional pressure and temperature sensors are used to track in-chamber conditions during operation.

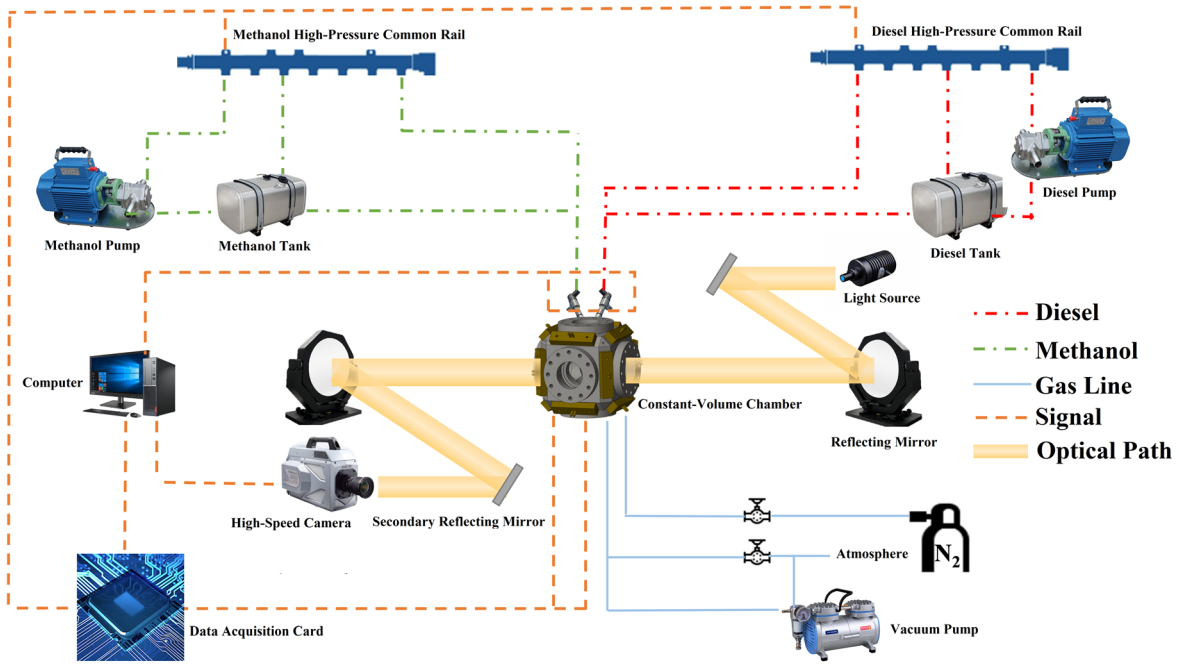

Figure 1. Diesel/methanol dual-fuel spray experimental system.

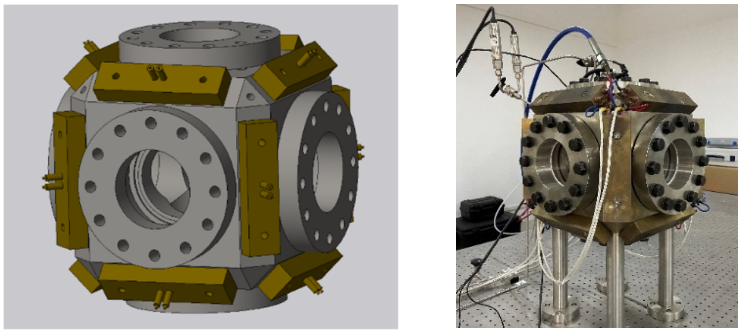

(**a**) (**b**)

Figure 2. Constant-volume chamber: (**a**) structural diagram and (**b**) physical photograph.

Spray images were acquired using a shadowgraph technique. The light source, mirrors, chamber windows, and camera formed a Z-shaped optical path, as illustrated in Figure 1. A Photron FASTCAM SA-Z high-speed camera (Photron, Tokyo, Japan) equipped with a Tokina AT-X Pro D 100 mm f/2.8 lens was operated at 20,000 fps, with a 1/200,000 s shutter speed and a 1024 × 1024 pixel resolution.

2.2. Dual-Fuel Spray Injection and Wall-Impingement Setup

The diesel/methanol dual-fuel injection assembly is shown in Figure 3. It consists of a diesel injector, a methanol injector, an injector clamping plate, and a metal mounting plug. Both injectors are Bosch units equipped with custom single-hole nozzles with a diameter of 0.2 mm. The axis angle between the two injectors is 15°, and the nozzle spacing is 12 mm. The injectors are fixed to the metal plug using a clamping plate and bolts, while polytetrafluoroethylene gaskets are placed at the interface to provide thermal resistance. The injector assembly is plane-mounted onto the constant-volume chamber to allow convenient installation and removal.

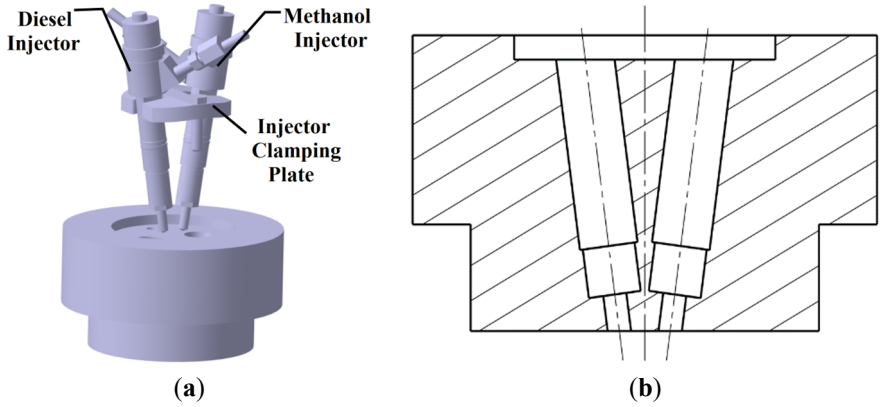

Figure 3. (**a**) Injector arrangement and (**b**) metal plug structure.

To investigate the wall-impingement behavior of diesel/methanol dual-fuel sprays, a spray wall-impact fixture was designed, as shown in Figure 4. The fixture consists of a mounting plug, a dovetail rail, a support plate, a sliding block, a circular impingement plate, and a support base. When installed on the constant-volume chamber, the center of the plate is aligned with the chamber's central axis. The fixture enables adjustment of the nozzle-to-wall distance from 20 to 70 mm and the wall angle from 0° to 70°, meeting the requirements of the dual-fuel spray wall-impingement experiments.

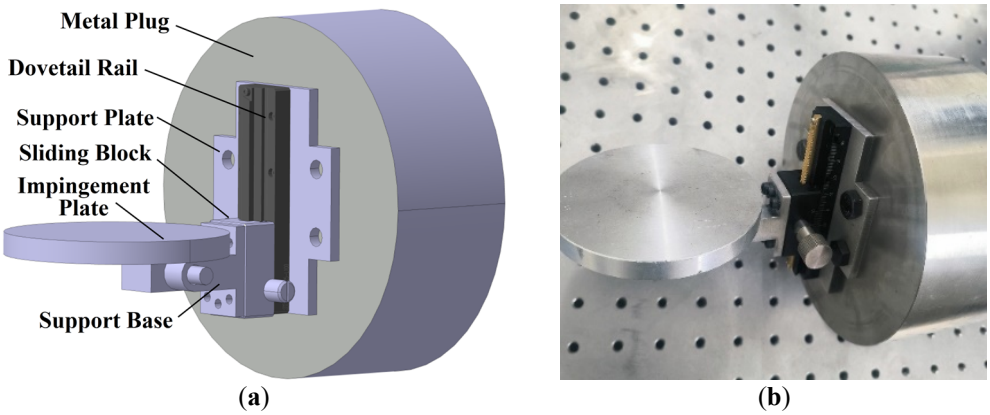

Figure 4. (**a**) Spray wall-impact plate assembly and (**b**) physical photograph.

2.3. Image Processing and Data Extraction

In the spray wall-impingement analysis, the characteristic parameters were defined based on the schematic shown in Figure 5a. After impacting the flat plate, the fuel spray spreads radially along the surface, and this radial extent is defined as the spreading radius (*R*). Meanwhile, small droplets lifted by vortical motion near the wall rise to a certain height above the surface, which is defined as the uplift height (*H*). These two parameters characterize the post-impingement behavior of the spray, indicating the extent of wall film distribution and the intensity of upward droplet motion driven by local flow structures. The wall-impingement distance (*H*w) is defined as the vertical distance from the nozzle exit to the wall-impingement point, and the wall-impingement angle (θ) is defined as the included angle between the horizontal reference line and the wall surface, as illustrated in Figure 5b.

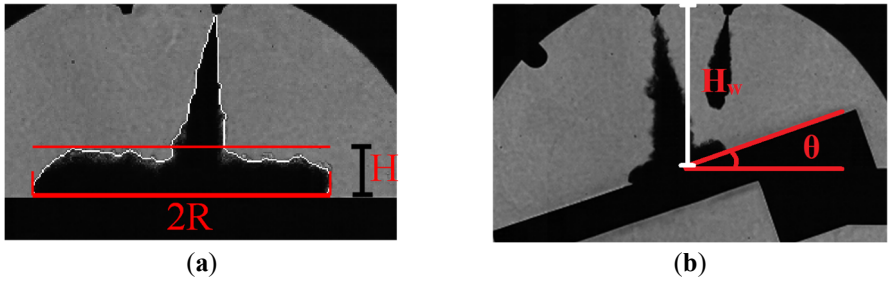

Figure 5. Definitions of wall-impingement geometry and characteristic parameters (a) Spray spreading radius (*R*) and uplift height (*H*)t; (b) Wall-impingement distance (*H*w) and angle (θ).

To reduce experimental uncertainty, each operating condition was tested three times, and the averaged values were used for parameter evaluation. Spray images were processed using a MATLAB-based algorithm developed in this study to extract the wall-impingement characteristics. The spray boundary used to extract R and H is defined as the outer contour of the background-subtracted shadowgraph image after Otsu-based binarization with median filtering and morphological hole removal, with further details provided in Ref. [31]. This contour-based criterion is applied consistently to all cases throughout the study.

Shadowgraph images and the extracted macroscopic metrics provide direct evidence of spray morphology, the formation and evolution of the apparent gas-phase region, and post-impingement spreading/uplift evolution. Mechanistic terms such as enhanced evaporation, intensified mixing, momentum loss, and secondary breakup are not measured directly; they are presented as reasonable inferences consistent with the observed image features and trends of R and H.

2.4. Experimental Conditions

In this study, n-dodecane with a purity of 99.99% was used as a diesel surrogate. To ensure consistent ambient conditions across tests, the chamber was purged after each run to remove residual fuel vapor and then refilled with fresh gas to the target pressure before the next injection. The spray strategy was kept constant throughout the study, with diesel injected first, followed 0.5 ms later by methanol, and the injection pressure for both fuels was maintained at 70 MPa. The diesel injection duration was 1.1 ms, corresponding to an injected mass of 8.1 mg, while the methanol injection duration was 1.5 ms, corresponding to an injected mass of 41.79 mg. In addition, both nozzle orifice diameters were 0.2 mm, and the ambient and fuel temperatures were controlled at 333 K and 293 K, respectively.

Under the fixed conditions described above, wall-impingement distance (H_w = 30, 40, 50, and 60 mm), and wall-impingement angle (θ = 0°, 20°, 40°, and 60°) were designated as the principal variables to systematically investigate their effects on the post-impingement spreading radius (R) and uplift height (H). The corresponding experimental configurations are summarized in Table 1.

Table 1. Experimental conditions for diesel/methanol dual-fuel spray wall-impingement.

Parameter	Methanol	Diesel
Nozzle diameter [mm]	0.2	
Ambient temperature [K]	333	
Fuel temperature [K]	293	
Ambient pressure [MPa]	3.0	
Injection interval [ms]	0.5	
Injection pressure [MPa]	70	70
Injection duration [ms]	1.5	1.1
Injected mass [mg]	41.79	8.1
Wall-impingement distance [mm]	30, 40, 50, 60	
Wall-impingement angle [°]	0, 20, 40, 60	

To distinguish inter-spray interaction from single-spray wall impingement, a single-injector methanol spray case was conducted as a limiting baseline under identical conditions. The difference between the dual-injection results and this baseline is attributed to inter-spray interaction.

3. Results and Discussion

3.1. Effect of Wall-Impingement Distance

The wall-impingement distance (H_w) governs the droplet impact momentum and the ensuing near-wall dispersion dynamics, thereby shaping the extent of fuel adhesion and its spatial distribution on the surface. Accordingly, diesel/methanol dual-fuel spray impingement experiments were conducted at four selected distances (30, 40, 50, and 60 mm) at θ = 0°. As illustrated in Figure 6, the left nozzle is used for diesel injection, while the right nozzle is used for methanol injection. t_{ASOI} denotes the time after start of injection (ASOI), where t_{ASOI} = 0 is defined as the first observable spray appearance in the shadowgraph images. For reference and to isolate the contribution of dual-fuel interactions, single-fuel methanol impingement tests were additionally performed under identical operating conditions.

Figure 6 presents the evolution of diesel/methanol dual-fuel sprays under different wall-impingement distances. With increasing impingement distance, a larger gas-phase region forms near the outer boundary of the

methanol spray before reaching the wall. After impingement, atomization and evaporation become more pronounced, which reduces the mixture concentration in the near-wall region.

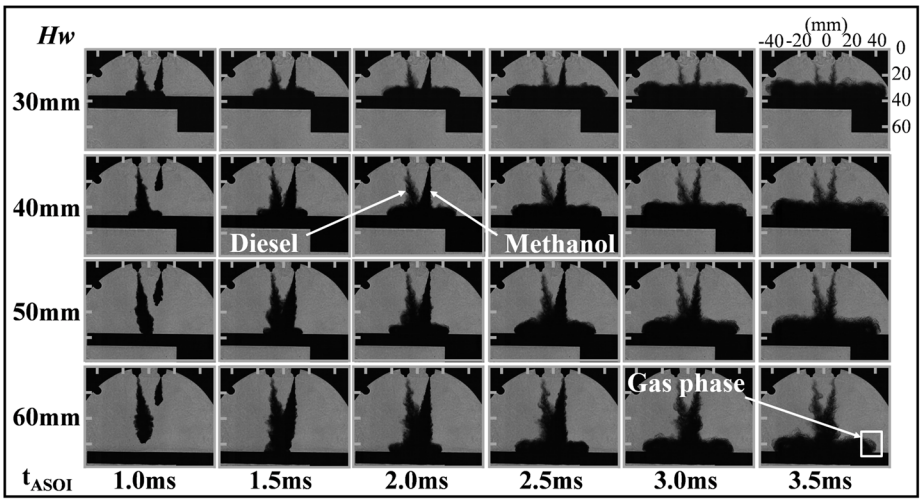

Figure 6. Diesel/methanol dual-fuel spray development at different wall-impingement distances.

Moreover, the impingement behavior of the dual-fuel spray changes with distance. At 30 and 40 mm, the diesel spray reaches the wall first, and the methanol spray subsequently impinges within the diesel-wetted region. In contrast, at 50 and 60 mm, the diesel and methanol sprays collide with each other before impinging on the wall. At these larger distances, inter-spray interaction enhances droplet breakup, and evaporation after impact is further intensified.

These results indicate that at 30 mm and 40 mm, droplet breakup and atomization are governed mainly by spray-wall interaction, whereas at 50 mm and 60 mm, the breakup process is jointly driven by inter-spray interaction and the spray-wall collision. The interaction between the diesel and methanol sprays substantially enhances droplet breakup and evaporation. The impingement distance extends the free-spray development before wall impact, promoting breakup and partial evaporation and thereby lowering the near-wall mixture concentration after impingement.

Figure 7 shows the evolution of the spreading radius of diesel/methanol dual-fuel sprays after wall impingement at different impingement distances. As the impingement distance increases, the spreading radius decreases, and the disparity between cases gradually narrows as time progresses. At t_{ASOI} = 1.8 ms, the spreading radius for 30 mm and 60 mm differs by 12.4 mm; by t_{ASOI} = 3.4 ms, the difference decreases to 5.9 mm. These observations indicate that a larger impingement distance reduces the momentum transferred to the wall at the moment of impact, leading to a markedly suppressed early-stage spreading. However, as the spray develops along the wall, the momentum decays, and the spreading rates for different distances converge, resulting in a substantially weaker influence of impingement distance during the later stage.

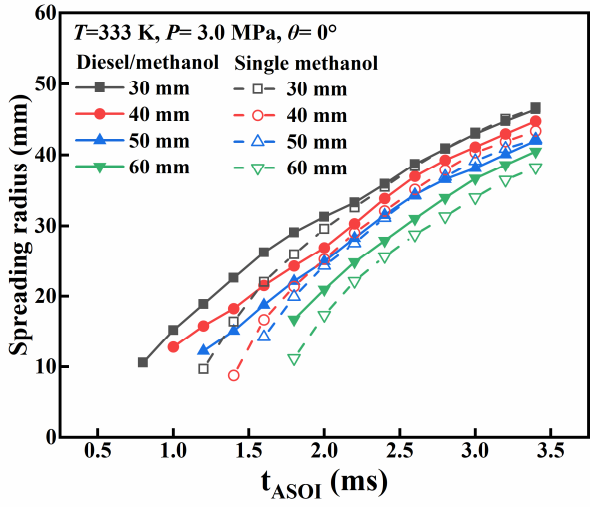

Figure 7. Spray spreading radius at different wall-impingement distances.

Compared with the diesel/methanol dual-fuel cases, the methanol single spray exhibits a smaller spreading radius before t_{ASOI} = 2.0 ms at all impingement distances, indicating weaker early-stage wall-parallel spreading. After t_{ASOI} = 2.0 ms, the spreading radii of the single- and dual-fuel sprays converge; however, their relative magnitude still depends strongly on the impingement distance, reflecting distinct spray-pray and spray-wall interaction pathways. For impingement distances of 30 mm, 40 mm, and 60 mm, the spreading radius of the methanol single spray remains smaller than that of the dual-fuel spray during the later stage. In the first two cases, the diesel spray reaches the wall first and spreads over the plate surface. The subsequently injected methanol spray contributes additional momentum during the later spreading process on the wall, resulting in a larger spreading radius for the dual-fuel spray. At 60 mm, substantial inter-spray collision and mixing occur before the sprays reach the wall, which elevates the overall momentum level of the dual-fuel jet. As a result, its spreading radius becomes larger than that of the methanol single-fuel spray. In contrast, at 50 mm, the methanol single spray exhibits a larger spreading radius than the dual-fuel spray in the later stage. This is because the methanol jet collides with the diesel jet immediately after the diesel spray contacts the wall, partially canceling the momentum and thereby weakening the spreading development of the dual-fuel spray.

Figure 8 illustrates the evolution of the uplift height of diesel/methanol dual-fuel sprays at different wall-impingement distances. Before t_{ASOI} = 2.0 ms, the uplift height decreases as the impingement distance increases, indicating that a larger distance weakens the near-wall vortical structures generated after impingement. As the spray continues to evolve, however, the uplift height no longer shows a monotonic dependence on impingement distance. This response reflects the coupled influence of spray impact velocity, post-impingement spreading, and the sequencing between inter-spray collision and spray-wall contact. These factors alter droplet breakup and atomization, thereby affecting the upward motion of droplets. Consequently, at later times, the uplift height is governed primarily by local flow structures and inter-spray interactions rather than by the impingement distance alone.

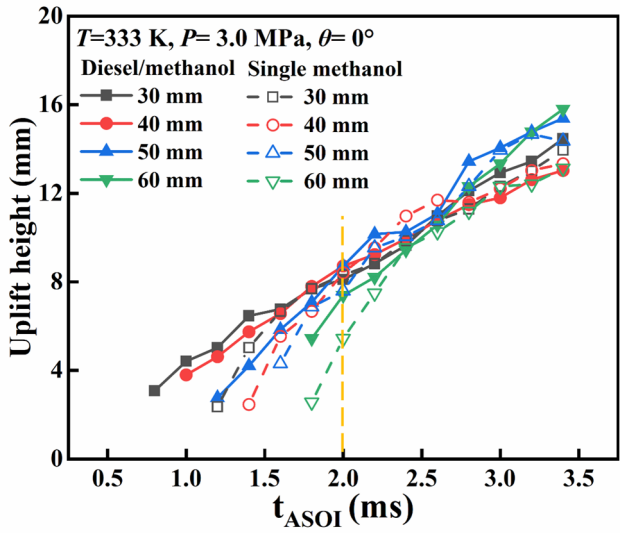

Figure 8. Spray uplift height at different wall-impingement distances.

3.2. Effect of Wall-Impingement Angle

The wall-impingement angle (θ) alters the incident momentum direction of the droplets, thereby influencing the post-impingement spreading and spatial distribution. Therefore, dual-fuel spray tests were further conducted at four wall-impingement angles (0°, 20°, 40°, and 60°) at H_w = 40 mm. Single-fuel methanol impingement tests were also performed under the same conditions.

Figure 9 shows the development of diesel/methanol dual-fuel sprays after wall impingement at different impingement angles. As the angle increases, the post-impingement spray distribution gradually shifts toward the lower-left region, and the entrainment vortex in this area becomes larger. This occurs because a larger impingement angle strengthens the guiding effect of the wall, causing the spray to travel along the inclined surface. As fuel continues to pile up in this region, the local spray momentum increases, enhancing the shear-induced entrainment and leading to the formation of a more pronounced vortex at the spray front.

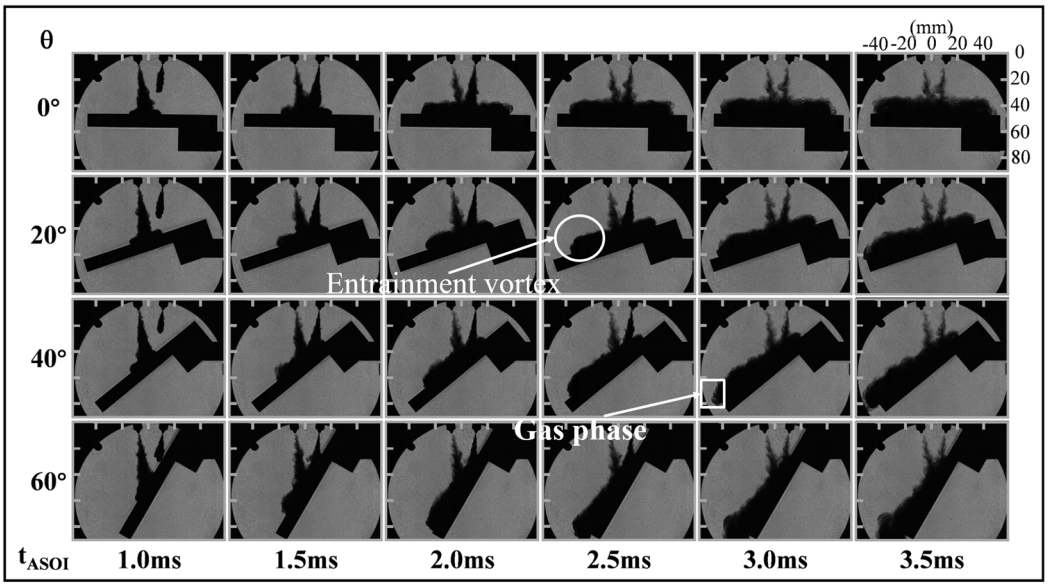

Figure 9. Diesel/methanol dual-fuel spray development at different wall-impingement angles.

The gas-phase region of the dual-fuel spray also changes with the impingement angle. At 0°, the gas-phase region is mainly located on the methanol-spray side to the right. As the angle increases, this region gradually shifts toward the lower-left direction along the wall. When the angle reaches 60°, the gas-phase region is concentrated near the vortex at the spray front. This is because, at large angles, droplet rebound near the impingement point becomes weaker, while the spray momentum and turbulence along the inclined surface increase, causing evaporation and entrainment to intensify around the front-end vortex.

Overall, increasing the impingement angle enhances the wall-guided deflection of the spray, resulting in a more concentrated distribution on the inclined side. Meanwhile, the gas-phase region progressively shifts from the methanol-spray side to the vortex region at the spray front.

Figure 10 shows the evolution of the spreading radius of diesel/methanol dual-fuel sprays at different impingement angles. Before t_{ASOI} = 2.0 ms, the spreading radius increases with the impingement angle. This is because a larger angle reduces the momentum loss of impact, allowing the spray to spread farther along the inclined wall. After the end of the injection, the spreading evolution exhibits a different dependence on the impingement angle. At an impingement angle of 0°, the spray spreads symmetrically to both sides. Although the momentum loss upon impact is larger for this case, the symmetric two-sided spreading accelerates the late-stage growth of the spreading radius, eventually surpassing that at 20°.

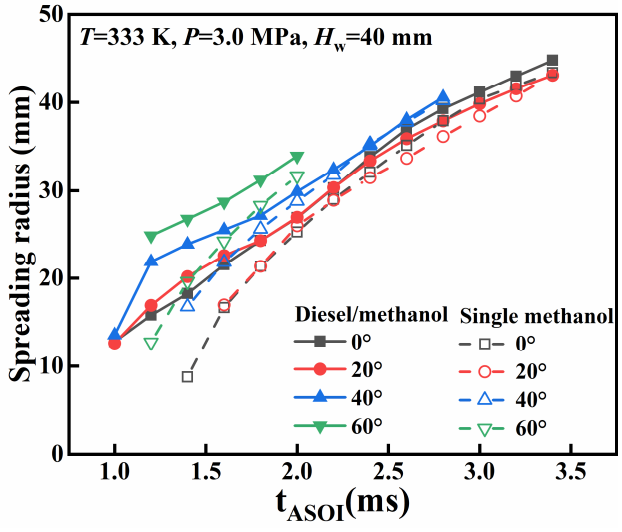

Figure 10. Spray spreading radius at different wall-impingement angles.

Compared with methanol single-fuel impingement, the dual-fuel sprays exhibit a larger spreading radius during the initial 2.0 ms, and the differences among angles are more pronounced. In the later stage, however, the

spreading radius of the dual-fuel and single-fuel sprays gradually converges. It indicates that the addition of diesel enhances the wall-directed spreading momentum in dual-fuel impingement, thereby increasing the sensitivity of the spreading radius to the impingement angle.

Figure 11 shows the temporal evolution of the uplift height of diesel/methanol dual-fuel sprays at different impingement angles. During the injection period, the uplift height exhibits a non-monotonic dependence on angle, increasing from 0° to 40° and then decreasing at 60°. After the injection ends, however, the uplift height increases monotonically with angle. This trend is attributed to the fact that at 40°, droplet rebound following impingement is more pronounced, leading to a comparatively larger uplift height during injection. In contrast, at 60°, the reduced momentum loss upon impact leads to the formation of a stronger entrainment vortex, which promotes a rapid increase in uplift height in the later stage.

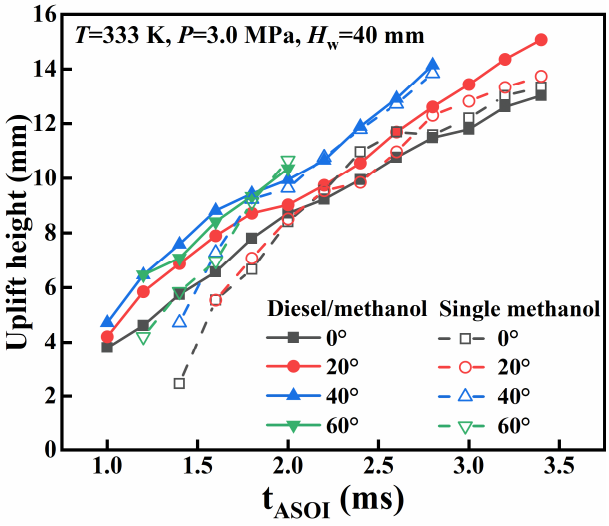

Figure 11. Spray uplift height at different wall-impingement angles.

Compared with dual-fuel sprays, methanol single-fuel sprays exhibit lower uplift heights during the injection period and display limited sensitivity to small variations in impingement angle; a marked increase is observed only when the angle rises from 20° to 40°. This difference is attributed to the stronger inter-spray interactions in the dual-fuel case, both before and after wall impact, which enhance droplet breakup and rebound, thereby amplifying the dependence of uplift height on impingement angle. Overall, the impingement angle exerts a stronger influence on the dual-fuel sprays, showing an increase-decrease trend during injection and a clear angle dependence afterward. In contrast, the methanol single-fuel sprays exhibit only weak sensitivity to angle variation within the small-angle range.

4. Conclusions

This study investigated the wall-impingement behavior of diesel/methanol dual-fuel sprays under varying impingement distances and angles, focusing on the post-impingement spreading and uplift characteristics. The results demonstrate that both geometric parameters strongly affect droplet momentum redistribution, spray–spray interaction, and near-wall vortex evolution, leading to distinct differences between dual-fuel and methanol single-fuel behaviors. The conclusions are as follows:

(1) Increasing the wall-impingement distance enlarges the gas-phase region near the outer boundary of the methanol spray before wall impact, leading to more pronounced atomization and evaporation after impingement and a lower mixture concentration near the wall. At short distances (30–40 mm), droplet breakup and atomization are dominated by spray-wall interaction, whereas at larger distances (50–60 mm), breakup is jointly governed by inter-spray collision and spray-wall impact. A larger impingement distance reduces the spreading radius and uplift height in the early stage, and its influence on spreading becomes progressively weaker as the wall-impingement process evolves.

(2) Increasing the impingement angle strengthens the wall-guided deflection of the spray, causing the dual-fuel spray to accumulate preferentially on the inclined side of the plate and shifting the gas-phase region from the methanol-spray side toward the front vortex. Compared with a single-fuel methanol spray, the presence of diesel in the dual-fuel configuration markedly amplifies the sensitivity of spreading radius and uplift height to impingement angle, resulting in stronger angle-dependent variation in near-wall spray evolution.

Author Contributions: H.S.: experimental planning, conceptualization; Z.Z.: supervision, review; C.L.: supervision, conceptual advice; M.L.: Methodology, Manuscript Writing; Y.Y.: experimental assistance; D.D.: funding acquisition; X.Z.: experiments analysis; Y.Z.: experimental assistance. All authors have read and agreed to the published version of the manuscript.

Funding: This work was supported by the National Natural Science Foundation of China (Grant No. 52301367) and the National Natural Science Foundation of China (Grant No. 52471340).

Institutional Review Board Statement: Not applicable.

Informed Consent Statement: Not applicable.

Data Availability Statement: Data will be made available on request.

Conflicts of Interest: The authors declare that they have no known competing financial interests or personal relationships that could have appeared to influence the work reported in this paper.

Use of AI and AI-Assisted Technologies: No AI tools were utilized for this paper.

References

1. Liu, H.; Yi, W.; Jalkanen, J.P.; Luo, Z.; Majamäki, E.; Matthias, V.; He, K. Atmospheric impacts and regulation framework of shipping emissions: Achievements, challenges and frontiers. *Fundam. Res.* **2024**, *5*, 1073.
2. Farkas, A.; Degiuli, N.; Martić, I; Vujanović, M. Greenhouse gas emissions reduction potential by using antifouling coatings in a maritime transport industry. *J. Clean. Prod.* **2021**, *295*, 126428.
3. Kontovas, C. Integration of air quality and climate change policies in shipping: The case of sulphur emissions regulation. *Mar. Policy* **2020**, *113*, 103815.
4. Parris, D.; Spinthiropoulos, K.; Ragazou, K.; Giovou, A.; Tsanaktsidis, C. Methanol, a plugin marine fuel for greenhouse gas reduction—A review. *Energies* **2024**, *17*, 605.
5. Xu, C.; Zhuang, Y.; Qian, Y.; Cho, H. Effect on the performance and emissions of methanol/diesel dual-fuel engine with different methanol injection positions. *Fuel* **2022**, *307*, 121868.
6. Dong, P.; Gao, J.; Liu, S.; Wang, J.; Zhang, X.; Wu, J.; Cui, Z. Ignition and combustion characteristics of ammonia applying an ignition chamber fueled by methanol and gasoline. *Energy* **2025**, *326*, 136280.
7. Karvounis, P.; Theotokatos, G.; Vlaskos, I.; Hatziapostolou, A. Methanol combustion characteristics in compression ignition engines: A critical review. *Energies* **2023**, *16*, 8069.
8. Yao, A.; Yao, C. Study of diesel/methanol dual fuel combustion in CI engines and its practice in China. *Int. J. Automot. Manuf. Mater.* **2023**, *2*, 2.
9. Yin, X.; Li, W.; Duan, H.; Duan, Q.; Kou, H.; Wang, Y.; Zeng, K. A comparative study on operating range and combustion characteristics of methanol/diesel dual direct injection engine with different methanol injection timings. *Fuel* **2023**, *334*, 126646.
10. Bao, G.; He, C.; Li, J. Effects of Different Methanol/Diesel Ratios on Engine Performance under Plateau Environment. *Int. J. Automot. Manuf. Mater.* **2025**, *4*, 2.
11. Huang, W.; Oguma, M.; Kinoshita, K.; Abe, Y.; Tanaka, K. Investigating Spray Characteristics of Synthetic Fuels: Comparative Analysis with Gasoline. *Int. J. Automot. Manuf. Mater.* **2024**, *3*, 2.
12. Gong, Y.; Liu, S.; Li, Y. Investigation on methanol spray characteristics. *Energy Fuels* **2007**, *21*, 2991–2997.
13. Wang, Y.; Dong, P.; Long, W.; Tian, J.; Wei, F.; Wang, Q.; Li, B. Characteristics of evaporating spray for direct injection methanol engine: Comparison between methanol and diesel spray. *Processes* **2022**, *10*, 1132.
14. Chen, Z.; Zhao, P.; Zhang, H.; Chen, H.; He, H.; Wu, J.; Lou, H. An optical study on the cross-spray characteristics and combustion flames of automobile engine fueled with diesel/methanol under various injection timings. *Energy* **2024**, *290*, 130286.
15. Wang, Q.; Wei, F.; Dong, P.; Xiao, G.; Cui, Z.; Tian, J.; Long, W. Visualization study on combustion characteristics of direct-injected hydrous methanol ignited by diesel in a constant volume combustion chamber. *Fuel* **2023**, *335*, 127063.
16. Li, Z.; Wang, Y.; Geng, H.; Zhen, X.; Liu, M.; Xu, S.; Li, C. Effects of diesel and methanol injection timing on combustion, performance, and emissions of a diesel engine fueled with directly injected methanol and pilot diesel. *Appl. Therm. Eng.* **2019**, *163*, 114234.
17. Wang, X.; Xia, T.; Li, H.; Dong, Q.; Qiao, Y.; Cheng, Q. Combustion characteristics of a methanol-diesel dual fuel engine with high-pressure direct injection. *Appl. Therm. Eng.* **2025**, *282*, 128748.
18. Sabathil, D.; Koenigstein, A.; Schaffner, P.; Fritzsche, J.; Doehler, A. The Influence of DISI Engine Operating Parameters on Particle Number Emissions. In Proceedings of the SAE World Congress, Rosemont, IL, USA, 13–14 September 2011.
19. Zhang, Z.; Long, W.; Cui, Z.; Dong, P.; Tian, J.; Tian, H.; Meng, X. Visualization study on the ignition and diffusion combustion process of liquid phase ammonia spray ignited by diesel jet in a constant volume vessel. *Energy Convers. Manag.* **2024**, *299*, 117889.

20. Dong, P.; Zhang, Y.; Ma, C.; Jin, Y.; Huang, R.; Zhai, C.; Tian, X. A geometric similarity analysis of high-temperature evaporating spray from multi-hole fuel injectors. *Int. Commun. Heat Mass Transf.* **2025**, *169*, 109889.
21. Wang, Q.; Guo, B.; Zhong, W.; Jiang, P.; Liu, X. Study on combustion and soot formation characteristics of RCCI engine with diesel mixed with PODE ignited gasoline. *Int. J. Automot. Manuf. Mater.* **2024**, *3*, 2.
22. Paul, W.; Paul, K.; Martin, O. Measures to Reduce Particulate Emissions from Gasoline DI engines. *SAE Int. J. Engines* **2011**, *4*, 1498–1512.
23. Chen, Z.; He, H.; Wu, J.; Wang, L.; Lou, H.; Zhao, P.; Chen, H. An experimental study the cross spray and combustion characteristics diesel and ammonia in a constant volume combustion chamber. *Energy* **2024**, *293*, 130733.
24. Li, K.; Ido, M.; Ogata, Y.; Nishida, K.; Shi, B.; Shimo, D. Effect of spray/wall interaction on diesel combustion and soot formation in two-dimensional piston cavity. *SAE Int. J. Engines* **2013**, *6*, 2061–2071.
25. Allocca, L.; Lazzaro, M.; Meccariello, G.; Montanaro, A. Schlieren visualization of a GDI spray impacting on a heated wall: Non-vaporizing and vaporizing evolutions. *Energy* **2016**, *108*, 93–98.
26. Yu, H.; Liang, X.; Shu, G.; Wang, Y.; Zhang, H. Experimental investigation on spray-wall impingement characteristics of n-butanol/diesel blended fuels. *Fuel* **2016**, *182*, 248–258.
27. Du, W.; Zhang, Q.; Bao, W.; Lou, J. Effects of injection pressure on spray structure after wall impingement. *Appl. Therm. Eng.* **2018**, *129*, 1212.
28. Wang, D.; Shi, Z.; Li, Y.; Yang, Z.; Chen, H.; Sun, C. Spray-wall interaction on n-dodecane spray combustion and soot formation under different wall temperatures. *Fuel* **2023**, *337*, 127180.
29. Liu, R.; Huang, L.; Yi, R.; Xia, J.; Zhang, J.; Feng, M.; Lu, X. Visualization on spray and flame characteristics of wall-impinging spray under marine diesel engine conditions. *Appl. Therm. Eng.* **2024**, *244*, 122655.
30. Zhang, Y.J.; Wei, Y.J.; Jamil, H.; Liu, S.H. Investigation of the behaviors of methanol spray impingement and wall wetting. *Appl. Sci.* **2022**, *12*, 12263.
31. Zhang, H. *Study on Spray Characteristics under Diesel/Methanol Dual Direct Injection Mode*; Wuhan University of Technology: Wuhan, China, 2025.